Inorg. Chem. **2007**, *46*, 196–207

Glycine- and Sarcosine-Based Models of Vanadate-Dependent Haloperoxidases in Sulfoxygenation Reactions

Cornelia Wikete,[†] Pingsong Wu,[†] Giuseppe Zampella,[‡] Luca De Gioia,[‡] Giulia Licini,[§] and Dieter Rehder*,[†]

Department Chemie, Universität Hamburg, 20146 Hamburg, Germany, Dipartimento di Biotechnologica, Universitá di Milano-Bicocca, 20106 Milano, Italy, and Dipartimento di Chimica Organica, Universitá degli Studi di Padova, 35131 Padova, Italy

Received August 14, 2006

Reaction of *R*-styreneoxide with glycine-*tert*-butylester yielded amino alcohols of the general formula $NR^1R^2R^3$, where R^1 = $CH_2COOtBu$ and R^2 = R^3 = 2-phenyl-2-hydroxyethyl ($H_2\mathbf{L_A}$); R^2 = 2-phenyl-2-hydroxyethyl and R^3 = 1-phenyl-2-hydroxyethyl ($H_2\mathbf{L_B}$); R^2 = H and R^3 = 2-phenyl-2-hydroxyethyl ($H\mathbf{L_C}$); and R^2 = H and R^3 = 1-phenyl-2-hydroxyethyl ($H\mathbf{L_D}$). The corresponding reaction with sarcosine-*tert*-butylester and subsequent hydrolysis provided the zwitterion $^+NH(CH_3)\{CH_2CHPh(OH)\}(CH_2CO_2^-)$, $H\mathbf{L_E^*}$ (asterisk refers to unprotected carboxylate). Reaction of these ligands with $VO(OiPr)_3$ in CH_2Cl_2 gave the oxovanadium(V) complexes [VO**L**($OiPr$)$_2$] and [VO$\mathbf{L}_2$($OiPr$)] (for $\mathbf{L_C}$ and $\mathbf{L_D}$) or, when reacted in the presence of MeOH, [VO**L**′(OMe)], where **L**′ represents the methyl ester of $\mathbf{L_A}$, $\mathbf{L_B}$, and $\mathbf{L_E}$. The crystal and molecular structures of *R*-H$\mathbf{L_C}$, *S*-H$\mathbf{L_D}$, *R*,*S*-H$\mathbf{L_E^*}$·H_2O, and Λ-[VO(*R*,*S*-$\mathbf{L_B'}$)OMe] have been determined. The complex [VO$\mathbf{L_B'}$(OMe)] contains vanadium in a distorted trigonal-bipyramidal array (τ = 0.72), the oxo group in the equatorial plane, and methoxide and N in the apical positions, and thus, it structurally models the active center of vanadate-dependent haloperoxidases. The structure and the bonding parameters, including a particularly long *d*(V–N) of 2.562 Å, are backed up by DFT calculations. The isolated oxovanadium(V) complexes and the in situ systems **L** + $VO(OiPr)_3$ catalyze the oxidation, by cumylhydroperoxide HO_2R', of prochiral sulfides (MeSPh, MeS*p*-Tol, PhSBn) to chiral sulfoxides plus some sulfone. The best results with respect to enantioselectivity (enantiomeric excess (ee) = 38%) were obtained with the system $VO(OiPr)_3$/$\mathbf{L_A}$, and the best selectivity with respect to sulfoxide (100%) was obtained with [VO$\mathbf{L_A}$($OiPr$)]. The reaction with the hexacoordinated [VO(OMe)(HOMe)$\mathbf{L_D^*}$] was very slow. Oxidation of PhSBn is faster than that of MeSPh and MeS*p*Tol. Turn-over numbers are up to 60 mol of sulfoxide mol^{-1} of catalyst h^{-1} (–20 °C). The unspectacular ee apparently is a consequence of flexibility of the active catalyst in solution, as shown by the ^{51}V NMR of the catalysts [VO**L**(OR)] and the oxo-peroxo intermediates [VO**L**(O_2R')]. As shown by DFT calculations, the peroxo ligand coordinates in the tilted end-on fashion in the axial or equatorial position (energy difference = 17.6 kJ/mol).

Introduction

The catalytic potential of vanadium was discovered in 1895 in the context of the use of vanadium pentoxide in the oxidation of toluene to benzaldehyde.[1] To date, a variety of oxidation reactions with peroxides as oxidizing agents and peroxovanadium compounds as catalysts or active intermediates in catalysis are known,[2] including the oxidation of organic sulfides (thioethers).[3,4] The oxidation of sulfides, which leads to chiral sulfoxides if prochiral sulfides and

* To whom correspondence should be addressed. E-mail: rehder@chemie.uni-hamburg.de.
[†] Universität Hamburg.
[‡] Universitá di Milano-Bicocca.
[§] Universitá degli Studi di Padova.

(1) (a) Walter, J. *J. Prakt. Chem.* **1885**, *51*, 107−111. (b) Alexander, J. *Chem. Ind.* **1929**, *48*, 871−878, 895−901.
(2) (a) Butler, A.; Clague, M. J.; Meister, G. E. *Chem. Rev.* **1994**, *94*, 625. (b) Hirao, T. *Chem. Rev.* **1997**, *97*, 2707. (c) Conte, V.; Di Furia, F.; Moro, S. *J. Phys. Org. Chem.* **1996**, *9*, 329−336.
(3) (a) Nakajima, K.; Kojima, M.; Kojima, K.; Fujita, J. *Bull. Chem. Soc. Jpn.* **1990**, *63*, 2620. (b) Bolm, C.; Bienewald, F. *Angew. Chem., Int. Ed. Engl.* **1995**, *34*, 2640. (c) Kagan, H. B. In *Asymmetric Oxidation of Sulfides*;: Ojima, I., Ed.; Wiley-VCH: New York, 2000; Chapter 6c. (d) Smith, T. S., II; Pecoraro, V. L. *Inorg. Chem.* **2002**, *41*, 6754−6780.
(4) Santoni, G.; Licini, G.; Rehder, D. *Chem.—Eur. J.* **2003**, *9*, 4700−4708.

10.1021/ic061534p CCC: $37.00
Published on Web 12/14/2006

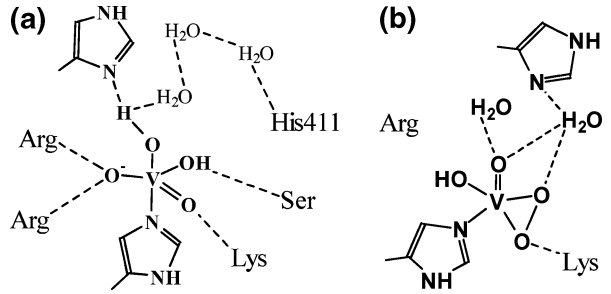

Figure 1. Native[11a] (a) and peroxo[12] (b) forms of the bromoperoxidase from *A. nodosum*. His411 is replaced by Phe in the chloroperoxidases from the fungus *Curvularia inaequalis*.[11b]

chiral catalyst systems are employed (eq 1) is reminiscent of the sulfide-peroxidase activity of vanadate-dependent haloperoxidases from marine macroalgae such as *Ascophyllum nodosum*, *Corallina pilulifera*, and *C. officinalis*.[5−7] Enantiopure sulfoxides are of prime interest because of their potential as chiral auxiliaries in organic syntheses,[3c,8,9] bioactive compounds,[10] and pharmaceuticals, such as Sulindac.

(1)

The active center of the vanadate-dependent haloperoxidases (VHPO) contains vanadate(V) covalently bonded to a histidine and in hydrogen-bonding contact with various amino acid side-chains from the surrounding protein pocket[11] (cf. Figure 1a). Vanadium is in a trigonal-bipyramidal array, with the Nϵ of His and an OH in the axial positions. In the intermediately formed peroxo- and hydroperoxo species, rearrangement toward a distorted tetragonal pyramid occurs, with the peroxo ligand in the side-on axial/equatorial position[12−14] (Figure 1b). To model the active center of the VHPO, we have employed the chiral amino alcohols depicted in Scheme 1 as ligands, derived from glycine (H_nL_{A-D}) and sarcosine (HL_E). The present results are an extension of earlier work,[4] where we have shown that related amino alcohols (without the carbonic acid function) form trigonal-bipyramidal oxovanadium(V) complexes that catalyze sulfoxygenation reactions.

Results and Discussion

Ligands. The *t*butyl forms of the ligands H_nL (cf. Scheme 1) were prepared by stirring *R*-styreneoxide and gylcine-*t*butylester or sarcosine-*t*butylester in silica gel for 6 days, adapting literature procedures for related amino alcohols.[15,16] The reaction course is displayed for the glycine derivatives in Scheme 2. The various components formed were separated and purified by flash chromatography on silica gel with hexane/acetic acid ester as the elutant. With a 1:1 ratio of the reactants, the yields were 20 (H_2L_A), 32 (HL_D), and 10% (HL_C), and at a ratio of 2:1 (styrene/glycine ester), they were 38 (H_2L_A) and 37% (HL_D). H_2L_B was obtained as a minor byproduct only. All of the ligands were recovered with the chiral carbons in their original (i.e., styreneoxide) configuration, and they were characterized by IR, ^{1}H, and ^{13}C NMR (see Supporting Information) and MS (see Scheme 3 for HL_D). Dependent on the cleavage of the styreneoxide in the 1,2- or 1,3-position, the phenyl group is adjacent to the OH (H_2L_A, one of the arms in H_2L_B, HL_C) or to N (one of the arms in H_2L_B, HL_D). For the latter case, this is clearly reflected in the multiplet structure of the ^{1}H NMR signal for {N-*CH*$_2$-COO*t*Bu} because of the interaction of the methylene protons with the phenyl group. Conversion of the *t*butyl forms of the ligands to the methyl esters H_nL' was achieved by re-esterification in methanol. The zwitterionic HL_E^* was obtained by saponification of the ester with KOH.

The ligands HL_C, HL_D, and HL_E^* have been structurally characterized. ORTEP plots are shown in Figure 2, and selected bonding parameters are collated in Table 1.

The bond distances and angles are in the expected range. The coordination environment of the ammonium-N in HL_E^* is almost tetrahedral (average CNC angle = 112.2°), and the N atom attains the *S* configuration. In the crystal lattice, ligands HL_C and HL_D occur in the form of pairs, kept together by intermolecular hydrogen bonds between the OH and N (2.836 and 2.864 Å). In the case of $HL_E^*\cdot H_2O$, chains are formed by linkages of carboxylate and hydroxyl through interstitial water molecules: *d*(carboxylate-O···OH$_2$) = 2.752 and *d*(H$_2$O···OH) = 2.648 Å (cf. Figure 3).

Oxovanadium complexes. The oxovanadium(V) complexes were prepared by reacting the ligands with VO(O*i*Pr)$_3$ in organic solvents, commonly, CH_2Cl_2 or MeOH. The

(5) Martinez, J. S.; Croll, G. L.; Tschirret-Guth, R. A.; Altenhoff, G.; Little, R. D.; Butler, A. *J. Am. Chem. Soc.* **2001**, *123*, 3289−3294.
(6) (a) ten Brink, H. B.; Holland, H. L.; Schoemaker, H. E.; van Lingen, H.; Wever, R. *Tetrahedron: Asymmetry* **1999**, *10*, 4563. (b) ten Brink, H. B.; Schoemaker, H. E.; Wever, R. *Eur. J. Biochem.* **2001**, *268*, 132.
(7) Andersson, M. A.; Allenmark, S. G. *Tetrahedron* **1998**, *54*, 15293.
(8) Andersen, K. K. In *The Chemistry of Sulfones and Sulfoxides*;: Patai, S., Rappoport, Z., Stirling, C. J. M., Eds.; John Wiley & Sons: Chichester, U.K., 1998; Chapters 3 and 16.
(9) Carreño, M. C. *Chem. Rev.* **1995**, *95*, 1717.
(10) (a) Holland, H. L.; Brown, F. M. *Tetrahedron: Asymmetry* **1998**, *9*, 535. (b) Conte, V.; di Furia, F.; Licini, G. *Appl. Catal. A* **1997**, *157*, 335.
(11) (a) Weyand, M.; Hecht, H.-J.; Kiess, M.; Liaud, M.-F.; Vilter, H.; Schomburg, D. *J. Mol. Biol.* **1999**, *293*, 595−611. (b) Messerschmidt, A.; Wever, R. *Proc. Natl. Acad. Sci. U.S.A.* **1996**, *93*, 392−396.
(12) Messerschmidt, A.; Prade, L.; Wever, R. *Biol. Chem.* **1997**, *378*, 309−315.
(13) Zampella, G.; Fantucci, P.; Pecoraro, V. L.; De Gioia, L. *J. Am. Chem. Soc.* **2005**, *127*, 953−960.
(14) Balcells, D.; Maseras, F.; Lledós, A. *J. Org. Chem.* **2003**, *68*, 4265−4274.
(15) (a) Kotsuki, H.; Shimanouchi, T.; Teraguchi, M.; Kataoka, M.; Tatsukawa, A.; Nishizawa, H. *Chem. Lett.* **1994**, 2159−2162. (b) Raubo, P.; Wicha, J. *Synlett.* **1993**, 25−26. (c) Bennett, F.; Patel, N. M.; Girijavallabhan, V. M.; Ganguly, A. K. *Synlett.* **1993**, 703−704.
(16) (a) Brine, G. A.; Sawyer, D. K.; Huang, P. T.; Stark, P. A.; Gaetano, K. D.; Carroll, F. I. *J. Hetrocycl. Chem.* **1992**, *29*, 1773−1779. (b) Pascal, M. L. *Bull. Soc. Chim.* **1960**, 435−442. (c) Zilkha, A.; Rappoport, S. *J. Org. Chem.* **1963**, *28*, 1105−1107. (d) Erhardt, P. W.; Woo, C. M.; Gorczynski, R. J.; Anderson, W. G. *J. Med. Chem.* **1982**, *25*, 1402−1407.

Scheme 1. Ligands Used in the Present Study[a]

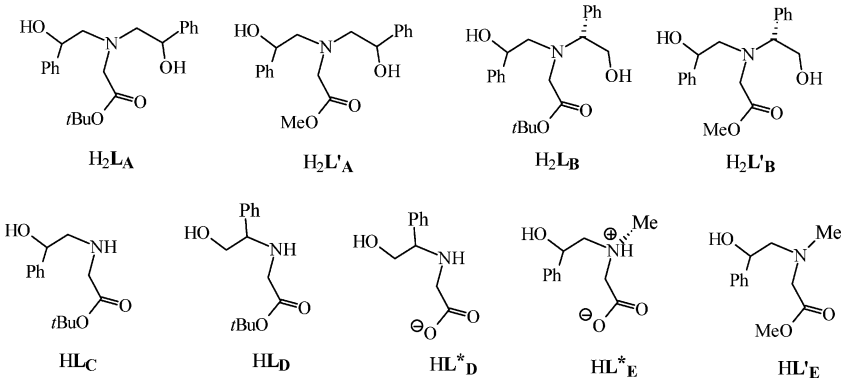

[a] A prime (′) indicates a methyl ester (unprimed = *t*butyl ester), and an asterisk (*) represents the unprotected carboxylate.

Scheme 2. Preparation of the *tert*-Butyl Forms of the Ligands

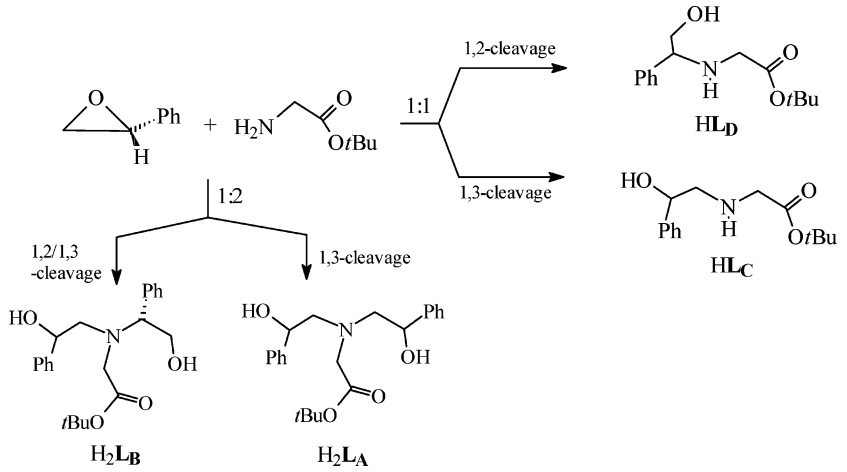

Scheme 3. Main Mass-Spectrometric Fragmentation Pattern of the Ligands (charges omitted) for H**L**$_{\mathbf{D}}$

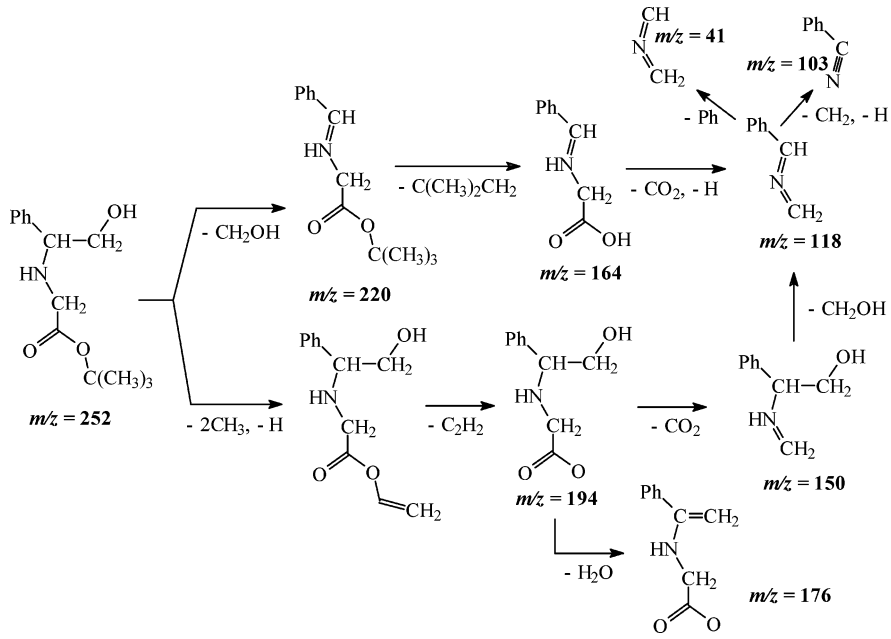

tridentate ligands $H_2\mathbf{L_A}$ and $H_2\mathbf{L_B}$, when reacted with $VO(OiPr)_3$ in dichloromethane, yield [VO(O*i*Pr)**L**] (eq 2a). In the presence of MeOH, the methoxy complexes [VO(OMe)**L**′] are obtained, and both the coordinated isopropoxo ligand and the dangling *tert*-butyl ester, undergo re-esterification (eq 2b). The reactions are slow and can be

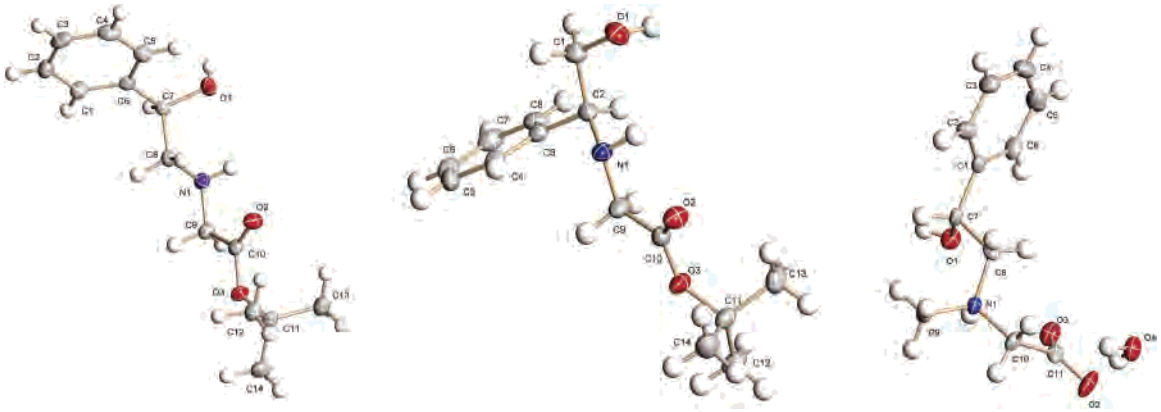

Figure 2. ORTEP plots (50% probability level) of, from left to right, *R*-H$\mathbf{L_C}$, *S*-H$\mathbf{L_D}$, and *R*,*S*-H$\mathbf{L_E^*}$·H_2O.

Table 1. Selected Bond Lengths (Å) and Angles (deg) for H$\mathbf{L_C}$, H$\mathbf{L_D}$, and H$\mathbf{L_E}$

	H$\mathbf{L_C}$		H$\mathbf{L_D}$		H$\mathbf{L_E^*}$	
d(C−N)					C9−N1	1.493(6)
d(C−N)	C8−N1	1.469(2)	C2−N1	1.4792(17)	C8−N1	1.496(6)
d(C−N)	C9−N1	1.462(2)	C9−N1	1.4655(17)	C10−N1	1.497(6)
d(C−C(OH))	C7−C8	1.514(2)	C1−C2	1.5234(19)	C7−C8	1.513(7)
d(C−C(OO*t*Bu))	C9−C10	1.521(2)	C9−C10	1.5073(19)	C10−C11	1.543(7)
d(C−O(carbox))	C10−O2	1.199(2)	C10−O2	1.2001(16)	C11−O3	1.242(6)
d(C−O(carbox))	C10−O3	1.339(2)	C10−O3	1.3418(16)	C11−O2	1.238(6)
d(C(*t*Bu)-O)	C11−O3	1.489(2)	C11−O3	1.4825(19)		
d(C−OH)	C7−O1	1.422(2)	C1−O1	1.4239(17)	C7−O1	1.410(6)
∠ at N	C8−N1−C9	114.84(14)	C9−N1−C2	111.33(12)	C9−N1−C8	113.6(4)
∠ at N					C9−N1−C10	110.8(4)
∠ at N					C8−N1−C10	112.1(4)
∠ at Cα	N1−C8−C7	109.25(14)	N1−C2−C1	108.87(13)	N1−C8−C7	111.7(4)
∠ at Cα	N1−C9−C10	115.44(15)	N1−C9−C10	111.52(12)	N1−C10−C11	111.3(4)
∠ at C(OH)	O1−C7−C8	107.55(14)	O1−C1−C2	113.42(13)	O1−C7−C8	106.4(4)
∠ at C(carbox)	O2−C10−O3	126.79(14)	O2−C10−O3	126.84(17)	O2−C11−O3	129.1(5)

followed by ^{51}V NMR spectroscopy: the signals at −68 ($VO(OiPr)_3$) or −625 ppm ($VO(OMe)(OiPr)_2$) are gradually replaced by those for the complexes, which appear at $\delta(^{51}V)$ values around −460 ppm (for further details, see below). In case of the bidentate ligands, H$\mathbf{L_C}$ and H$\mathbf{L_D}$, mixtures of [VO(O*i*Pr)$\mathbf{L}_2$] and [$VO(OiPr)_2\mathbf{L}$] are obtained in CH_2Cl_2 (eq 3); they are clearly distinguished by their ^{51}V NMR chemical shifts (around −460 for the bis(ligand) and −510 ppm for the mono(ligand) complexes). The sarcosine derived zwitterionic ligand H$\mathbf{L_E^*}$ forms the complex [VO(OMe)$\mathbf{L_E^*}$] (eq 4), along with some [$VO(OMe)_3$] ($\delta(^{51}V) = -557$ ppm[17]).

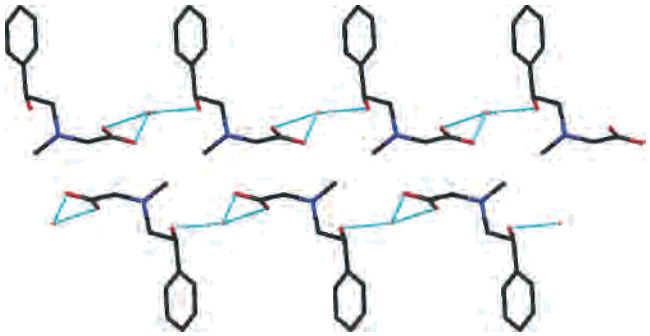

Figure 3. Orientation of the ligands H$\mathbf{L_E^*}$ along the crystallographic *a* axis. Hydrogen bonds, linking carboxylate and hydroxyl via water molecules, are represented by dashed lines.

$$H_2\mathbf{L} + [VO(OiPr)_3] \rightarrow [VO(OiPr)\mathbf{L}] + 2HOiPr\ (\mathbf{L} = \mathbf{L_A}\ \text{and}\ \mathbf{L_B}) \quad (2a)$$

$$[VO(OiPr)\mathbf{L}] + MeOH \rightarrow [VO(OMe)\mathbf{L'}] + HOiPr + HOtBu\ (\mathbf{L} = \mathbf{L_A}\ \text{and}\ \mathbf{L_B}) \quad (2b)$$

$$H\mathbf{L} + [VO(OiPr)_3] \rightarrow [VO(OiPr)_2\mathbf{L}]/[VO(OiPr)\mathbf{L}_2] + HOiPr\ (\mathbf{L} = \mathbf{L_C}\ \text{and}\ \mathbf{L_D}) \quad (3)$$

$$H\mathbf{L_E^*} + [VO(OiPr)_3] + MeOH \rightarrow [VO(OMe)\mathbf{L_E^*}] + HOiPr\ (+ [VO(OMe)_3]) \quad (4)$$

The ligand H$\mathbf{L_D}$ has also been converted to the potassium carboxylate $K^+[H\mathbf{L_D^*}]^-$ (Scheme 4). Subsequent reaction with $VO(OiPr)_3$ lead to the formation of [VO(HOMe)(OMe)-$\mathbf{L_D^*}$], with $\mathbf{L_D^*}$ coordinating in the tridentate manner (i.e., including carboxylate). As shown by the $\Delta\nu = \nu_{asym} - \nu_{sym} = 311\ cm^{-1}$, the carboxylate coordinates in the monodentate fashion. The suggested octahedral formulation provided in

(17) (a) Priebsch, W.; Rehder, D. *Inorg. Chem.* **1990**, *29*, 3013−3019. (b) Rehder, D.; Weidemann, C.; Duch, A.; Priebsch, W. *Inorg. Chem.* **1988**, *27*, 584−587.

Scheme 4. Saponification of Ligand H$\mathbf{L_D}$ and Reaction with VO(O*i*Pr)$_3$ in Methanol to Form [VO(HOMe)(OMe)H$\mathbf{L_D^*}$]

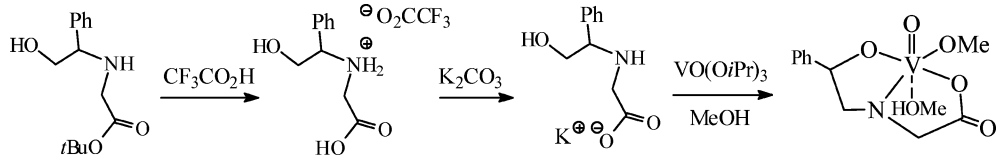

Table 2. ^{51}V NMR Chemical Shifts Relative to $VOCl_3$[a]

[VO(OMe)$\mathbf{L'_A}$] −449, −470	[VO(OMe)$\mathbf{L'_B}$] −451, −471	[VO(O*i*Pr)($\mathbf{L_C}$)$_2$] −467	[VO(O*i*Pr)($\mathbf{L_D}$)$_2$] −450, −479	[VO(OMe)$\mathbf{L_E^*}$] −448, −465
		[VO(O*i*Pr)$_2\mathbf{L_C}$] −502	[VO(O*i*Pr)$_2\mathbf{L_D}$] −520	
			[VO(HOMe)(OMe)$\mathbf{L_D^*}$] −544	

[a] In CH_2Cl_2 or (for methoxo complexes (primed ligands)) MeOH.

Scheme 4, with an additional methanol ligand weakly bonded in the axial position, is based on the chemical shift $\delta(^{51}V) = -544$ ppm.

^{51}V NMR spectral results are summarized in Table 2. Electronic factors influencing ^{51}V shielding in V^V (d^0) complexes are, inter alia, the coordination number, cn (increased shielding with decreasing cn), and the overall electronegativity, en, of the ligand set (increasing shielding with increasing en).[17] The range observed here with the pentacoordinated complexes containing an O_4N donor set including chelating ligands is well in accord with expectations.[17−19] The spacious iso-propoxo ligand gives rise to a particularly high shielding;[17,20] the signals at −502 and −520 ppm have therefore been assigned to the complexes [VO(O*i*Pr)$_2$**L**], containing two iso-propoxo ligands. The $\delta(^{51}V)$ for the complex formed with $\mathbf{L_D^*}$, −544 ppm, is tentatively assigned to an octahedral complex, in analogy to similar complexes.[21] For the complexes [VO(OR)**L**], R = Me or *i*Pr, **L** = $\mathbf{L'_A}$, $\mathbf{L'_B}$, $\mathbf{L_D}$, and $\mathbf{L_E^*}$, two signals of comparable integral intensity are observed, separated by ∼20 ppm. Two sets of signals are also observed in the ^{1}H NMR spectra. Possible explanations for the presence of two species in solution are (i) diastereomers (where applicable),[21,22] (ii) equilibria between monomeric and dimeric (or oligomeric) complexes,[4,17,23] and (iii) flexibility with respect to the coordination geometry [square-pyramidal vs trigonal-bipyramidal, tbp (iiia)] and the arrangement of the ligands [equatorial vs axial position of the doubly bonded oxo group for tbp (iiib)]. Case i can be ruled out because the $\Delta\delta$ is too large for diastereomers present in solution.[21,22] Association to dimers or oligomers (case ii) should be temperature dependent; no substantial temperature dependence of $\delta(^{51}V)$ has been observed in the temperature range of −20 to +50 °C. On the basis of the structure determination of Λ-[VO(OMe)(R,S-$\mathbf{L'_B}$)] (vide infra) and the $\delta(^{51}V)$ values of −464 ± 15 ppm (Table 2), we assume a (slightly distorted) tbp geometry for the complexes in solution, with the oxo group mutually in the equatorial and axial positions (i.e., case (iiib; Scheme 5). DFT calculations (see below) indicate, that the energy difference between the two iiib isomers amounts to a few kilojoules per mole only.

Scheme 5. Proposed Structural Isomers of [VO(OMe)(R,S-$\mathbf{L'_B}$)] in Solution

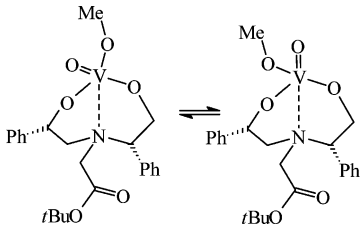

The structure of Λ-[(OMe)VO(R,S-$\mathbf{L'_B}$)] as determined by X-ray crystallography and DFT calculations is represented in Figure 5, selected structure parameters are given in Table 3. The complex attains the structure of a distorted trigonal bipyramid; the τ factor amounts to 0.72. Vanadium is 0.377 Å above the plane defined by the oxo group (O6) and the two alcoholate functions O1 and O2; the methoxy group and the amine-N are in the axis, slightly deviating from linearity (angle O5−V−N = 167.80(2)°). The overall geometry thus compares to that previously observed for related oxovanadium complexes.[4] Bonding parameters are, in general, similar to those reported for, for example, [VO(OMe)L^1] (H_2L^1 = R,R-bis(2-phenylethanol)-R-1-phenylethylamine) except for the distance d(V−N), which is 2.291(2) Å in the latter complex[4] and 2.562(5) Å in [VO(OMe)(R,S-$\mathbf{L'_B}$)]. The additional weakening of the d(V−N) trans to the methoxide may come about by a steric influence imparted by the phenyl group in α position to the N; d(V−N) is still in the range found for coordinated amines subjected to the trans influence of an oxo functional ligand.[24] The bonding parameters, including d(V−N), are also in good agreement with those obtained from the DFT calculations (Table 3). The shortest

(18) Howarth, O. W. *Prog. NMR Spectrosc.* **1991**, *22*, 453−485.
(19) Crans, D. C.; Felty, R. A.; Chen, H.; Eckert, H.; Das, N. *Inorg. Chem.* **1994**, *33*, 2427−2438.
(20) Paulsen, K.; Rehder, D.; Thoennes, D. *Z. Naturforsch.* **1978**, *33a*, 834−839.
(21) Fulwood, R.; Schmidt, H.; Rehder, D. *J. Chem. Soc., Chem. Commun.* **1995**, 1443−1444.
(22) Weidemann, C.; Priebsch, W.; Rehder, D. *Chem. Ber.* **1989**, *122*, 235−243.
(23) Hillerns, F.; Olbrich, F.; Behrens, U.; Rehder, D. *Angew. Chem., Int. Ed. Engl.* **1992**, *31*, 447−448.
(24) (a) Launay, J. P.; Jeannin, Y.; Daoudi, M. *Inorg. Chem.* **1985**, *24*, 1052−1059. (b) Mahroof-Tahir, M.; Keramidas, A. D.; Goldfarb, R. B.; Anderson, O. P.; Miller, M. M.; Crans, D. C. *Inorg. Chem.* **1997**, *36*, 1657−1668. (c) Bashirpoor, M.; Schmidt, H.; Schulzke, C.; Rehder, D. *Chem. Ber./Recl.* **1997**, *130*, 651−657.

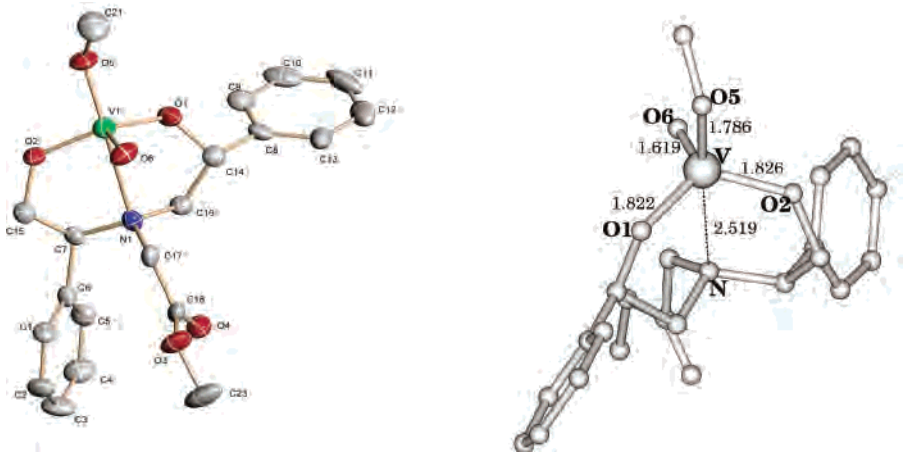

Figure 4. (left) ORTEP drawing (50% probability level) of Λ-[(OMe)VO(R,S-$\mathbf{L'_B}$)]. (right) Calculated (DFT) structure (for details see below).

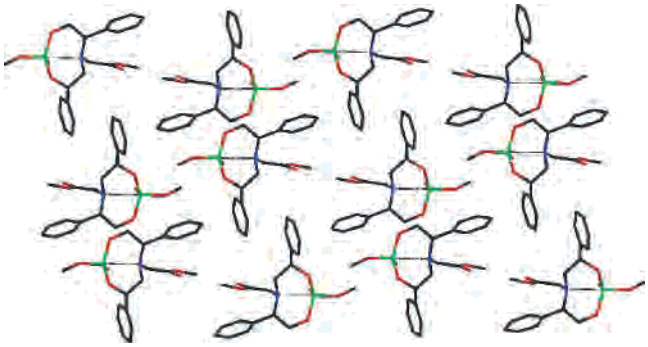

Figure 5. Packing scheme (along the crystallographic *b* axis) for Λ-[V(OMe)O(R,S-$\mathbf{L'_B}$)].

Table 3. Selected Bond Lengths (Å) and Angles (deg) for Λ-[VO(OMe)(*R*,*S*-$\mathbf{L'_B}$)] Obtained from the X-ray Structure Determination and the Structure Optimized on the Basis of DFT Calculations[a]

	[VO(OMe)$\mathbf{L'_B}$]		H$\mathbf{L_C}$/H$\mathbf{L_D}$
	X-ray results	DFT results	X-ray results
V−O6	1.590(5)	1.619	
V−O5	1.749(4)	1.786	
V−O1	1.807(5)	1.822	
V−O2	1.808(5)	1.826	
V−N	2.562(5)	2.519	
N−C17	1.470(8)	1.467	1.462(2) ($\mathbf{L_C}$), 1.4655(17) ($\mathbf{L_D}$)
N−C16	1.485(8)	1.481	1.469(2) ($\mathbf{L_C}$)
N−C7	1.502(8)	1.509	1.4792(17) ($\mathbf{L_D}$)
O1−C14	1.423(7)	1.412	1.422(2) ($\mathbf{L_C}$)
O2−C15	1.418(7)	1.412	1.4239(12) ($\mathbf{L_D}$)
O5−V−N1	167.80(2)	171.76	
O1−V−O2	124.30(2)	118.13	
O1−V−O6	109.30(3)	115.74	
O2−V−O6	112.60(3)	113.50	
O5−V−O6	106.00(3)	103.81	
N−V−O6	85.90(2)	84.43	
O1−V−N	73.21(19)	75.18	
O2−V−N	74.83(18)	74.75	
N−C17−C18	117.5(6)	116.05	115.44(15) ($\mathbf{L_C}$), 111.52(12) ($\mathbf{L_D}$)
O1−C14−C16	106.4(5)	107.36	107.55(14) ($\mathbf{L_C}$)
O2−C15−C7	109.1(5)	111.00	113.42(13) ($\mathbf{L_D}$)

[a] Corresponding X-ray data for the free ligands H$\mathbf{L_C}$ and H$\mathbf{L_D}$ are included for comparison.

intramolecular contact, between the oxo group and the amine-N, is 2.915 Å. The shortest intermolecular contacts (between phenyl carbons) are 3.46 Å; a packing Scheme is provided in Figure 5.

Scheme 6. Overall Reaction Scheme for V-Catalyzed Sulfoxygenation[a]

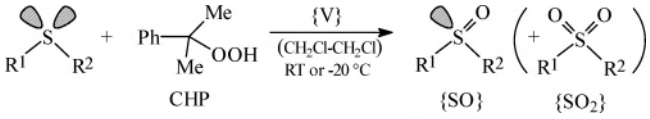

[a] R^1/R^2 = Me/Ph; Me/p-Tol; Me/Bn. {V} = VO(O*i*Pr)$_3$ + H$_n$**L** or [VO(O*i*Pr)**L**].

Table 4. Oxidation of MeSPh with Catalysts Based on $\mathbf{L_C}$- and $\mathbf{L_D}$-Type Ligands at Ambient Temperature[a]

catalyst	catalyst/MeSPh/CHP	conversion (%) after 10 min/6 h	{SO}/{SO$_2$} after 10 min/6 h
VO(O*i*Pr)$_3$ + H$\mathbf{L_D}$	1:10:10	80/100	79:21/78:22
	1:100:100	77/94	97:3/91:9
[VO(O*i*Pr)$_2$$\mathbf{L_D}$]	1:10:10	54/100	99:1/96:4
	1:10:20	84[b]	88:12
[VO(OMe)$\mathbf{L_D^*}$]	1:10:10	25[c]	100:0
[VO(O*i*Pr)$_2$$\mathbf{L_C}$]	1:10:10	80[b]	94:6
	1:10:20	79/100	20:80/3:97

[a] For abbreviations see Scheme 6, and for the ligands, see Scheme 1. [b] Reaction was completed after 50 min (100% conversion). [c] Very slow reaction (95% conversion after 19 h).

Sulfide Oxygenation Catalysis. The overall scheme for the oxidation (by cumylhydroperoxide, CHP) of prochiral sulfides in the presence of a vanadium catalyst {V} is displayed in Scheme 6, which also includes the abbreviations used in the following discussion. The catalyst was either employed in the form of the genuine complex or in situ as a mixture of VO(O*i*Pr)$_3$ plus ligand. Common (optimized) {V}/sulfide/CHP ratios were 1:10:10 at initial concentrations of sulfide and CHP = 0.1 M. Reaction temperatures were room temp or −20 °C. Product analysis was carried out by ^{1}H NMR, GC, and HPLC (see Experimental Section).

Selected results for MeSPh oxygenation employing $\mathbf{L_C}$- and $\mathbf{L_D}$-type ligands under different reaction conditions are collected in Table 4. An excess of CHP over sulfide results in increased production of sulfone at the expense of sulfoxide, a decrease of the mol % of the catalyst from 10 to 1% usually resulted in slightly slower reactions and nonquantitative conversion into products, even if better sulfoxide/sulfone ratios were obtained (Table 4, entry 2). Neither $\mathbf{L_C}$- nor $\mathbf{L_D}$-

Table 5. Oxidation of MeS*p*Tol and BnSPh with $\mathbf{L_A}$- and $\mathbf{L_D}$-Based Catalysts at −20 °C and at Room Temperature[a]

entry	catalyst (temp)	substrate	reaction (100% conversion)	{SO}/{SO}$_2$	excess of the *R* enantiomer (%)
1	$H_2\mathbf{L_A}$ + VO(O*i*Pr)$_3$ (room temp)	MeS*p*Tol	10 min	98:2	8.6
2	$H_2\mathbf{L_A}$ + VO(O*i*Pr)$_3$ (−20 °C)	MeS*p*Tol	2 h	93:7	37.9
3	[VO(O*i*Pr)$\mathbf{L_A}$] (−20 °C)	MeS*p*Tol	2 h	100:0	29.7
4	H$\mathbf{L_D}$ + VO(O*i*Pr)$_3$ (−20 °C)	MeS*p*Tol	2.5 h	92:8	1.5
5	$H_2\mathbf{L_A}$ + VO(O*i*Pr)$_3$ (−20 °C)	BnSPh	20 min	96:4	36.7
6	H$\mathbf{L_D}$ + VO(O*i*Pr)$_3$ (−20 °C)	BnSPh	5 h	100:0	0.7

[a] The catalyst/sulfide/CHP ratio was 1:10:10 in all cases; the initial concentrations for sulfide and CHP were 0.1 M. For the in situ systems, ligand and VO(O*i*Pr)$_3$ were employed in equimolar amounts.

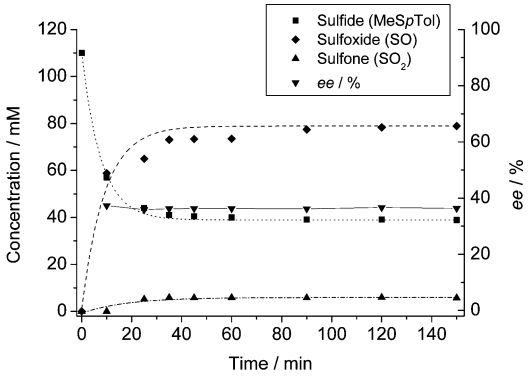

Figure 6. Time course of the oxidation of MeS*p*Tol with CHP in the presence of the catalyst system $H_2\mathbf{L_A}$ + VO(O*i*Pr)$_3$ at −20 °C.

based catalyst systems gave rise to stereoselective oxygenation. Corresponding results were observed in the oxidation of MeS*p*Tol. The complex [VO(HOMe)(OMe)$\mathbf{L_D^*}$] containing the deprotected and thus tridentate ligand (cf. Scheme 4) was also employed as a catalyst in the oxidation of MeSPh. Although selectivity was very good (only sulfoxide formed), reaction times were exceedingly slow (95% conversion after 19 h), and again no stereoselectivity was observed. We have therefore carried out the majority of our investigations without deprotecting the ligands.

More promising results with respect to the stereoselective sulfoxygenation were obtained with the $\mathbf{L_A}$-based catalyst systems and are listed, together with the results for $\mathbf{L_D}$ at low temperature, in Table 5. Figure 6 provides a graphical representation of the reaction course for MeS*p*Tol at −20 °C. The results indicate that the chiral ligand $\mathbf{L_A}$ is notably more effective and affords the sulfoxides with discrete enantiomeric excess (ee) values. The ee values substantially improve upon working at lower reaction temperature, both with the preformed catalyst [VO(O*i*Pr)$\mathbf{L_A}$] (entry 3) and the in situ system based on ligand $\mathbf{L_A}$ (entry 2). On the other hand, at −20 °C, the intact complex [VO(O*i*Pr)$\mathbf{L_A}$] provides a higher selectivity than the in situ system (entry 3 vs entry 2). Ligand $\mathbf{L_D}$ did not afford any significant stereoselection, and the reactions were slower (entries 4 and 6), indicating the beneficial effect of the presence of two alkoxy binding sites on the ligand, as provided by ligand $\mathbf{L_A}$. Finally, reaction rates for the oxidation of the sulfide with the in situ system $H_2\mathbf{L_A}$ + VO(O*i*Pr)$_3$ at −20 °C is considerably faster for benzyl-phenylsulfide (entry 5) than for methyl-*p*-tolylsulfide, even though comparable ee values are obtained. This latter observation is noteworthy, as is the fact that reaction with BnSPh is much faster than with MeS*p*Tol (compare entries 2 and 5), despite the slightly lower nucleophilicity of BnSPh.

Peroxo Intermediates. The unspectecular enantiomeric excess in our catalytically conducted sulfide oxidations supposedly is predominantly a consequence of the nonrigidity of the catalysts in solution. Insight into the reaction course, and thus the intermediates formed, was provided by ^{51}V and ^{1}H NMR analysis of the oxidation of methyl-phenylsulfide (MeSPh) by CHP with the complex [VO(O*i*Pr)$\mathbf{L_A}$] as catalyst. A 0.01 M solution of the vanadium complex in dichloroethane shows two resonances in the ^{51}V NMR at −452 and −470 ppm in an approximate ratio of 1:1, corresponding to the two diastereomers depicted in Scheme 5 (vide supra). Upon addition of CHP, the color changes from brown to orange, and two new signals appear at −521 and −540 ppm with about the same integral intensities, which we assign to the peroxo complexes on the basis of the well-established fact that coordination of peroxide increases shielding.[17,25] Upon the addition of the sulfide, the signals for the peroxo intermediates disappear, and those of the catalyst reappear together with two new signals assigned to a cumyl-alkoxo complex (Scheme 7). The increase of shielding on going from [VO(O*i*Pr)$\mathbf{L_A}$] to [VO(Ocumyl)-$\mathbf{L_A}$] is a consequence of the more pronounced steric requirement of the cumyl group.[17,26] In parallel to the ^{51}V NMR results, the ^{1}H NMR signal for the methyl protons of CHP (1.62 ppm) experience a downfield coordination shift of 0.12 ppm upon addition of the catalyst. After the addition of the sulfide, the signals appear at 1.46 ppm, corresponding to the cumyl-alkoxide. Concomitantly, a doublet at 1.07 ppm for 2-propanol, which is set free, is observed.

Following the results of DFT calculations (next section), we have formulated, in Scheme 7, the peroxo intermediate

(25) Andersson, I.; Garzsás, A.; Kerezsi, C.; Tóth, I.; Pettersson, L. *Dalton Trans*. **2005**, 3658−3666 and references to related topics therein.
(26) Hillerns, F.; Rehder, D. *Chem. Ber.* **1991**, *124*, 2249−2254.

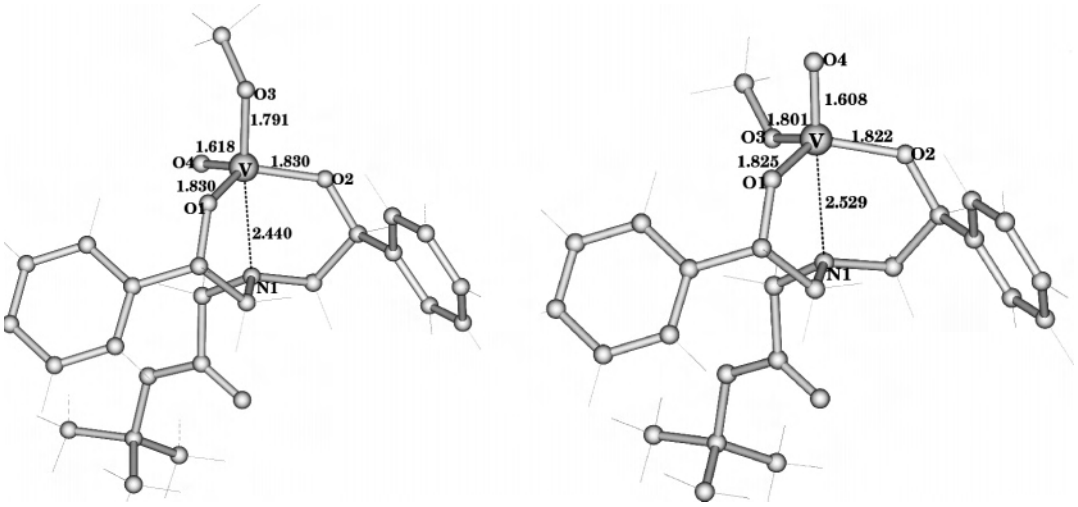

Figure 7. DFT-optimized structure of [VO(OMe)$\mathbf{L_A}$] isomers (distances in angstroms).

Scheme 7. Reaction Steps for the Catalysis by [VO(O*i*Pr)$\mathbf{L_A}$] Identified by ^{1}H and ^{51}V NMR

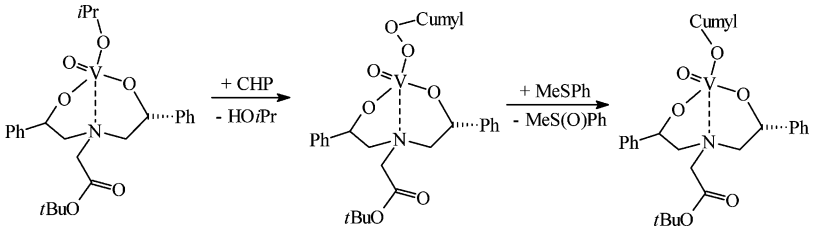

with the peroxide coordinated in the bent end-on mode in an axial position, in contrast to the structurally characterized vanadium complex [VO(OO*t*Bu)(dipic)(H_2O)] (dipic = 2,6-dipicolinate(2−)), for which X-ray results[27] indicate the (slightly asymmetrical) side-on coordination of the organic peroxo ligand in an equatorial position of an octahedral complex.

DFT Calculations. Initially, to determine if the adopted level of theory was suited to describe this class of compounds, we optimized the structure of [VO(OMe)$\mathbf{L'_B}$], for which X-ray diffraction data have been collected in this work (Figure 4 and Table 3). It turned out that the overall structure, as well as the bonding parameters (Table 3), are nicely reproduced by DFT calculations. Notably, also the long and unusual V−N distance is very well backed up by DFT calculations (2.562 and 2.519 Å in the X-ray and DFT structures, respectively), indicating that the adopted level of theory can be used to confidently describe the structural properties of this class of compounds.

Once we validated the computational approach, we investigated by DFT the structural features of vanadium complex [VO(OMe)$\mathbf{L_A}$], related to [VO(O*i*Pr)$\mathbf{L_A}$], which is characterized by the most interesting catalytic features (Table 5). The DFT structures corresponding to the isomers of [VO(OMe)$\mathbf{L_A}$], featuring the OMe group in the axial or equatorial position, are shown in Figure 7.

Interestingly, the [VO(OMe)$_{ax}\mathbf{L_A}$] species is characterized by a significantly shorter V−N bond distance than that of the [VO(OMe)$_{eq}\mathbf{L_A}$] isomer (2.440 and 2.529 Å, respectively) because of the destabilization of the V−N bond by the oxo group in trans, consistent with previous results obtained on models of the vanadate-dependent haloperoxidases cofactor.[28] The strong effect on the V−N bond length exerted by the ligand in trans indicates also that the potential energy surface associated to V−N bond stretching is quite flat. Comparison of the computed energy values for [VO(OMe)$_{ax}\mathbf{L_A}$] and [VO(OMe)$_{eq}\mathbf{L_A}$] indicates that the former is more stable by 4.2 kJ mol^{-1}.

To shed some light on the catalytic properties of the complex formed from [VO(OR)$\mathbf{L_A}$] and cumylhydroperoxide (HO_2R'), we investigated, by DFT, the structural features of the peroxo isomers [VO$\mathbf{L_A}$(O_2R')] (Figure 8). In [VO$\mathbf{L_A}$-(O_2R')$_{ax}$], the V−N bond distance is almost 0.2 Å shorter than that in [VO$\mathbf{L_A}$(O_2R')$_{eq}$], confirming the strong trans influence of the oxo group. [VO$\mathbf{L_A}$(O_2R')$_{ax}$] is more stable than [VO$\mathbf{L_A}$(O_2R')$_{eq}$] by 17.6 kJ mol^{-1}. The ratio of the two isomers of the active peroxo intermediate, as determined from the ^{51}V NMR spectrum (δ = −521 and −540), is 1:2.8, and that for the precatalyst [VO(OMe)$\mathbf{L'_A}$] (δ = −449 and −470 ppm) is 1.7:1. The ratio does not change significantly in the relevant temperature range investigated (−20 to +25 °C). As we have shown previously, on the basis of variable-temperature and EXSY spectroscopy,[4] there is exchange between the isomers on the millisecond scale. Interestingly, in both isomers the peroxo moiety is bound in an end-on fashion, whereas side-on species turned out to be unstable and spontaneously converted to the corresponding end-on forms. This observation highlights a possible key difference with the active enzymatic form, in which the peroxo group is bound in a side-on fashion. In particular, the end-on

(27) Mimoun, H.; Chaumette, P.; Mignard, M.; Saussine, L.; Fischer, J.; Weiss, R. *Nouv. J. Chim.* **1983**, *7*, 467−475.

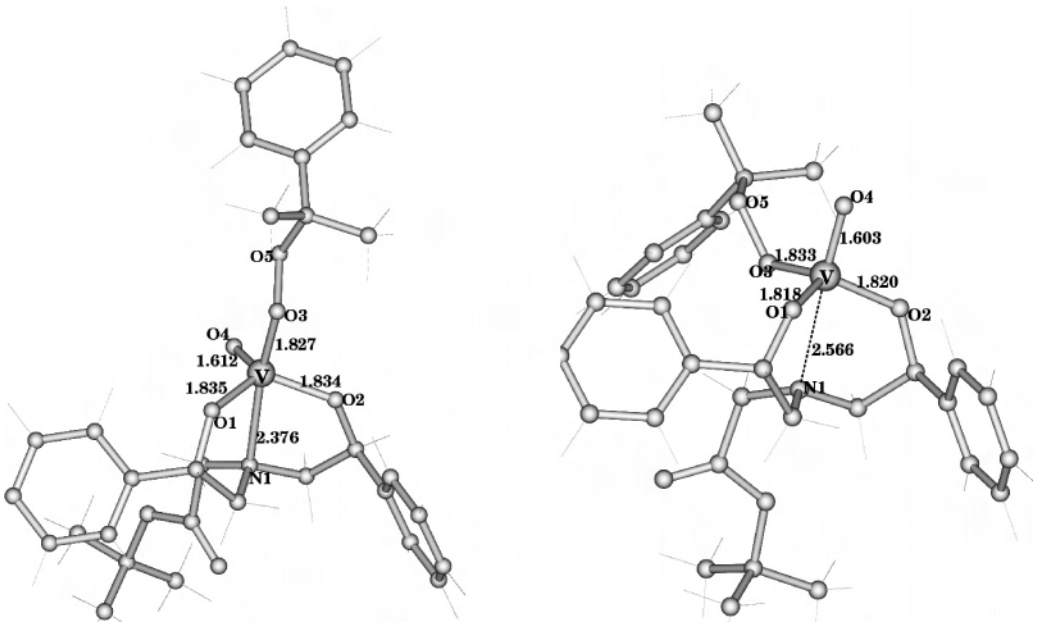

Figure 8. DFT-optimized structure of [VO$\mathbf{L_A}$(O_2R′)] isomers (distances in angstroms).

coordination predicted by DFT calculations is consistent with the steric requirement of the cumyl moiety and the high conformational mobility of the peroxo group in the catalytically active form; a characteristic that is expected to disfavor enantioselectivity.

Conclusion

Chiral mono- and diethanolamines, H**L** and H_2**L**, derived from glycine-*tert*-butyl ester and, in one case, from sarcosine, have been prepared by reaction of the O-protected amino acid with *R*-styreneoxide. The reaction of H_n**L** with VO(O*i*Pr)$_3$ leads to complexes of composition [VO(O*i*Pr)**L**] or, in the presence of methanol, [VO(OMe)**L**′], where **L**′ stands for the methyl ester of the glycine-derived ligand. As shown by X-ray diffraction studies and backed up by DFT calculations, the pentacoordinated oxovanadium(V) complexes adopt the slightly distorted trigonal-bipyramidal geometry ($\tau = 0.72$) and thus structurally model the active centers of vanadate-dependent haloperoxidases (VHPO). In the solid state, the equatorial position is the preferred one for the oxo group (as in the VHPO). The energy difference between [VO_{eq}(OR)L] and [VO_{ax}(OR)L] amounts to a few kilojoules per mole only. Consequently, as shown by ^{51}V NMR, there are the two isomers present in solution.

The complexes and the in situ systems (ligand + VO(O*i*Pr)$_3$) also model the sulfide-peroxidase activity of the VHPO (i.e., they catalyze the oxidation, by cumylhydroperoxide, of prochiral sulfides to chiral sulfoxides and, in most cases, some sulfone). The most efficient system with respect to selectivity (100% of sulfoxide) is the complex [VO(O*i*Pr)$\mathbf{L_A}$] ($H_2\mathbf{L_A}$ = bis(2-hydroxy-2-phenylethyl)glycine-*tert*-butylester), and the most efficient with respect to ee is the in situ system $\mathbf{L_A}$ + VO(O*i*Pr)$_3$. However, even with the latter catalyst and at optimized conditions (−20 °C, benzyl-phenylsulfide as substrate), the ee does not surmount 37%, reflecting the fluctunality of the intermediately formed procatalyst [VO(O*i*Pr)$\mathbf{L_A}$] and catalyst [VO(OOcumyl)$\mathbf{L_A}$], again shown by ^{51}V NMR. According to DFT calculations, the organic peroxo ligand coordinates in an end-on fashion, preferentially in the axial position. Turn-overs are up to 60 mol of sulfoxide mol^{-1} of catalyst h^{-1}. Deprotection of the ligand to provide an additional coordinating function and thus a more rigid complex, drastically reduces yields, as shown for the complex with the ligands $\mathbf{L_D}$/$\mathbf{L_D^*}$.

Experimental Section

Materials and Methods. The following starting materials were obtained from commercial sources (Sigma, Fluka) and were used without further purification: VO(O*i*Pr)$_3$, *R*-styreneoxide, glycine-*tert*-butyl ester, sarcosine-*tert*-butyl ester, sulfides, Pirkle alcohol [*R*-(−)-1-(9-anthryl)-2,2,2-trifluoroethanol], cumyl hydroperoxide (CHP). CHP, containing 16% cumene, was stored at 0 °C over 4 Å molecular sieves. Silica gel 60 (0.040−0.063 mm) was purchased from Merck. Solvents were dried, degassed, and stored under nitrogen. The preparation of the vanadium complexes was carried out using Schlenk techniques. The isolated and dried complexes are stable in air.

Elemental analyses were performed with a Heraeus CHN−O-Rapid analyzer. IR spectra were obtained in solution in KBr cuvettes or in KBr pellets on a Perkin-Elmer FT-IR spectrometer 1720XFT. NMR spectra were scanned on a Bruker AM 400 spectrometer with the usual parameter settings. ^{51}V NMR chemical shifts are quoted relative to $VOCl_3$ ($\delta = 0$). For the collection of FAB mass spectral data, a VG analytical mass spectrometer 70−250S, equipped with a xenon source, was employed. *m*-Nitrobenzyl alcohol was used as a matrix.

Sulfoxygenation Reactions. The catalytically conducted sulfoxygenations were performed at room temperature (RT) and −20 °C. For the reactions at RT, catalyst, CHP, and sulfide were successively dissolved in $CDCl_3$ (MeS*p*Tol) or CD_2Cl_2 (other sulfides) in an NMR tube under nitrogen, and NMR spectra were collected every 10 min until complete disappearance of the signals for CHP. The ratio of sulfoxide/sulfone was determined from the integral intensities of the ^{1}H NMR signals of the methyl (MeSPh

Table 6. Crystal Structure and Refinement Data

	HL_C	HL_D	$HL_E^*\cdot H_2O$	$[VO(OMe)(L'_B)]$
empirical formula	$C_{14}H_{21}NO_3$	$C_{14}H_{21}NO_3$	$C_{11}H_{17}NO_4$	$C_{20}H_{24}NO_6V$
mol mass (g/mol)	251.32	251.32	227.26	425.34
space group	$P2_12_12_1$	$P2_12_12_1$	$P2_1/n$	$P2_1$
a (Å)	6.4111(6)	5.8537(14)	5.396(2)	10.9385(9)
b (Å)	10.9482(10)	10.394(2)	7.990(3)	6.9591(5)
c (Å)	19.4735(18)	23.032(5)	26.351(10)	14.0081(11)
β (deg)			92.038(8)	107.452(2)
V (Å^3)	1366.8(2)	1401.4(6)	1135.2(8)	1017.24(14)
Z	4	4	4	2
D_{calcd} (g/mL)	1.221	1.191	1.330	1.389
μ (mm^{-1})	0.085	0.083	0.101	0.523
F(000)	544	544	488	444
cryst size (mm^3)	0.58 × 0.12 × 0.10	0.80 × 0.19 × 0.14	0.34 × 0.10 × 0.07	0.14 × 0.10 × 0.05
θ range (deg)	2.09−27.48	1.77−27.50	3.83−25.00	1.52−25.02
reflns collected	16 408	16 699	7411	10 441
data/restraints/params	1831/0/171	3207/2/174	1345/4/160	3586/1/258
GOF on F^2	0.901	0.995	0.909	0.825
R values ($I < 2\sigma I$)				
R1	0.0340	0.0399	0.0720	0.0476
wR2	0.0569	0.0515	0.1198	0.0947
R values (all data)				
R1	0.0479	0.0592	0.1384	0.0910
wR2	0.0596	0.0539	0.1399	0.1544
excess electron density max/min (e Å^{-3})	0.146/−0.144	0.149/−0.177	0.169/−0.211	0.317/−0.344

and MeS*p*Tol) or methylene protons (BnSPh). For the determination of the ee values, 5 equiv of Pirkle alcohol were added, and the ratio of the two diastereomeric sulfide−Pirkle adducts was determined by integration of the ^{1}H NMR resonances for the alkyl protons of the sulfide. Reactions at −20 °C were conducted in 1 mL reactors under a N_2 atmosphere. Sulfide (0.110 mmol), catalyst (0.011 mmol), and 0.07 mmol of the internal standard benzophenone were dissolved in 1,2-dichloroethane and cooled to −20 °C; 0.110 mmol of CHP was added with stirring (for other molar ratios of the reactants see the respective section in Results and Discussion). At defined time intervals, 50 μL aliquots of the reaction mixture were removed and immediately quenched by addition of an excess of dibutylsulfide, and the composition was analyzed by GC (to determine the ratio sulfoxide/sulfone) and HPLC (to determine the ee).

Quantitative product analyses for the catalytic reactions conducted at −20 °C were carried out with a Hewlett-Packard 5890 series II chromatograph, equipped with a capillary column with a FFAP EC-1000 stationary phase (30 m × 0.25 mm, film thickness of 0.25 μm) under the following conditions: initial temp of 55 °C for 1 min, rate of 15 °C per min, final temp of 200 °C for 30 min. The ee values for the sulfoxides were determined by HPLC with a Shimadzu LC-10AT chromatograph, UV Shimadzu SPD-10A (λ = 241 nm) detector, and a C-R5A Shimadzu Chromatopac integrator. The chromatograph was equipped with a chiral column, packed with Lichrosorb S100, *R*,*R*-diaminocyclohexane, DNB spherical 250 × 4 mm. A mixture of *n*-hexane/2-propanol (9:1) was employed as the elutant with a flow rate of 0.6 mL min^{-1} and a pressure of 17 kg cm^{-2}.

X-ray Structure Determinations. Data collections for single-crystal structure determinations were carried out at 153(2) K with a SMART APEX CCD Bruker diffractometer (graphite monochromator, Mo Kα irradiation, λ = 0.71073 Å). Frames were read out with the program SAINT; absorption corrections were carried out with SADABS. The program XPREP was used for the determination of the space group. SHELXS-97 and SHELXL-97 were employed for phase problems and structure refinement. Hydrogen atoms not participating in hydrogen bonds were placed into calculated positions, and the other hydrogens were located in the Fourier map. For structure and refinement data, see Table 6.

DFT Calculations. DFT calculations have been carried out using the pure functional BP86[29] or the hybrid B3-LYP[30] functional and a valence triple-ζ basis set with polarization on all atoms (TZVP).[31] All calculations have been carried out with the TURBOMOLE 5.7 suite,[32] applying the resolution-of-identity technique.[33] Free-energy (G) values were obtained from the electronic SCF energy by considering three contributions to the total partition function (Q), namely, q(translational), q(rotational), and q(vibrational), under the assumption that Q may be written as the product of such terms.[34] To evaluate enthalpy and entropy contributions, the values of temperature, pressure, and the scaling factor for the SCF wavenumbers have been set to 298.15 K, 10^2 kPa, and 0.9914, respectively. Rotations have been treated classically and vibrational modes have been described according to the harmonic approximation.

Preparation of Ligands. *tert*-Butyl-2-{bis-(*R*-2-hydroxy-2-phenylethyl)amino}acetate (H_2L_A), *tert*-Butyl-2-(*R*-2-hydroxy-1-phenylethyl)-2-(*R*-hydroxy-1-phenylethyl)aminoacetate (H_2L_B), *tert*-Butyl-2-(*R*-2-hydroxy-2-phenylethyl)aminoacetate (HL_C), and *tert*-Butyl-2-(*S*-2-hydroxy-1-phenylethyl)aminoacetate (HL_D). (See ref 15a for the preparation of more basic amino alcohols.) Silica gel (9.18 g, 0.15 mol) in a 100 mL round flask was treated with 1.5 mL (10.9 mmol) of *tert*-butylglycinate and 2.09 mL (18.3 mmol) of *R*-styreneoxide; the mixture was stirred at room temp for 6 days. The reaction mixture was poured on top of a silica gel column and separated by flash chromatography, starting with 7:3 hexane/acetic acid ester. The polarity of the elutant was gradually increased to a ratio of 1:2. H_2L_A was recovered as the first fraction as, after removal of the solvent with a rotary evaporator and drying

(28) Zampella, G.; Kravitz, J. Y.; Webster, C. E.; Fantucci, P.; Hall, M. B.; Carlson, H. A.; Pecoraro, V. L.; De Gioia, L. *Inorg. Chem.* **2004**, *43*, 4127.
(29) (a)Becke, A. D. *Phys. Rev. A.* **1998**, *38*, 3098. (b) Perdew, J. P. *Phys. Rev. B.* **1986**, *33*, 8822.
(30) Lee, C.; Yang, W.; Parr, R. G. *Phys. Rev. B* **1988**, *37*, 785−789.
(31) Schafer, A.; Huber, C.; Ahlrichs, R. *J. Chem. Phys.* **1994**, *100*, 5829.
(32) Ahlrichs, R.; Bar, M.; Haser, M.; Horn, H.; Kolmel, C. *Chem. Phys. Lett.* **1989**, *162*, 165.
(33) Eichkorn, K.; Weigend, F.; Treutler, O.; Ahlrichs, R. *Theor. Chem. Acc.* **1997**, *97*, 119.
(34) Jensen F. *Introduction to Computational Chemistry*; John Wiley & Sons Ltd.: Chichester, U.K., 1999.

over $CaCl_2$, a light yellow oil. R_f: 0.36 (1.5:1 hexane/acetic acid ester). Yield: 1.27 g (37.7%). $H_2\mathbf{L_B}$ was isolated from the second fraction in small and impure amounts only and characterized via its oxovanadium(V) complex (see below). $H\mathbf{L_C}$ and $H\mathbf{L_D}$, obtained from the third and forth fraction, were recrystallized from 1:2 H_2O/MeOH to form colorless needles with R_f values (1.5/1 hexane/acetic acid ester) of 0.09 and 0.31, respectively. The two isomeric ligands were obtained in yields of 0.45 (19.8%, $H\mathbf{L_C}$) and 0.84 g (36.7%, $H\mathbf{L_D}$).

The ligands were characterized by IR, ^{1}H NMR, ^{13}C NMR, MS, and elemental analyses (for details, see Supporting Information).

2-{*N*-(*R*-2-hydroxy-2-phenylethyl)}-*N*-methylaminoacetate Hydrate, $HL^*_E\cdot H_2O$. Sarcosine *tert*-butylester hydrochloride (0.74 g, 4 mmol) was dissolved in 2.5 mL of ethanol, and the pH was adjusted to 8 with NaOH. One milliliter (8 mmol) of *R*-styreneoxide was slowly added, and the mixture was stirred under reflux for 5 days. After it was cooled to room temperature, the reaction mixture was extracted with 30 mL of chloroform. The aqueous layer was slowly evaporated to yield colorless needles of $\mathbf{HL^*_E}$ suitable for X-ray crystallography. IR (KBr, cm^{-1}): ν(OH) 3435; ν(CH) 3063 (aryl), 2957 (alkyl); ν(N−CH_2) 2789; ν($^+$NH) 2425; ν(COO^-) 1631 (asym), 1325 (sym); ν(C═C ring) 1494; δ(CH) 1457 (alkyl), 762 and 703 (aryl); δ(COH) 1325; ν(CN) 1244; ν(CO)1158 and 1059.

Preparation of Complexes. [VO(O*i*Pr)$\mathbf{L_A}$] and [VO(OMe)$\mathbf{L'_A}$]. Ligand $H_2\mathbf{L_A}$ (0.19 g, 0.51 mmol) was dissolved in 4 mL of anhydrous CH_2Cl_2 and treated dropwise with 3 mL of a CH_2Cl_2 solution of 0.12 g (0.49 mmol) VO(O*i*Pr)$_3$. The yellow solution was stirred at room temperature for 1 h to yield, after evaporation of the solvent in vacuo, a viscous yellow oil. Efforts to isolate the complex in solid form failed. ^{1}H NMR (CD_2Cl_2): δ 7.41−7.21 (m, 40H, aromatic), 6.14−6.10 (dd, 3.3, 11.0, 2H, CH_2−C*H*(Ph)−OH (isomer 1)), 5.69−5.65 (dd, 3.7, 11.3, 4H, CH_2−C*H*(Ph)−OH (isomer 2)), 5.47−5.38 (sept., 6.1, 2H, V−O−C*H*(CH_3)$_3$), 4.19−4.15 (d, 18, 2H, N−CH_2−COO(*t*Bu)), 3.81−3.76 (d, 18, 2H, N−CH_2−COO(*t*Bu)), 3.70−3.63 (ddd, 3.7, 10.6, 12.6, 6H, N−CH_2−CH (isomer 1)), 3.47−3.42 (ddd, 3.2, 7.5, 12.9, 4H, N−CH_2−CH (isomer 2). ^{51}V NMR (CD_2Cl_2 (integral)): δ −448 (1.00), −471 (0.98).

[VO(OMe)$\mathbf{L'_A}$] was obtained from [VO(O*i*Pr)$\mathbf{L_A}$] by quantitative re-esterification in anhydrous methanol. After the mixture was stirred for 3 days at room temp, the green-yellow solid complex was recovered by filtration, washed with $CHCl_3$, and dried in vacuo. Yield: 0.123 g (59% with respect to the reactants for [VO(O*i*Pr)-$\mathbf{L_A}$]). IR (KBr, cm^{-1}): ν(OH) 3436; ν(aryl-H) 3062, 3029; ν(C−H) 2984, 2932; ν(C═O) 1656, 1599; ν(C═C ring) 1494; δ(C−H) 1451, 1409; δ(CH_3), δ(COH) 1370; δ(C−N) 1271; ν(C−O), ν-(C−OC) 1156, 1057, 1026; ν(V═O) 977; δ(aryl-H) 758, 701. ^{1}H NMR ($CDCl_3$): δ 7.48−7.28 (m, aromatic, 6.24−6.20 (dd, 3.3, 10.9, 2H, CH_2−C*H*(Ph)−OH (isomer 1)), 5.61−5.58 (dd, 3.1, 9.1, CH_2−C*H*(Ph)−OH (isomer 2)), 5.28 (s, 3H, V−O−CH_3), 4.27−4.23 (d, 18, 2H, N−CH_2−COOCH_3), 3.79−3.75 (dd, 3.4, 12.6, N−CH_2−CH (isomer 1)), 3.60 (s, 3H, −COOCH_3), 3.20−3.14 (dd, 5.6, 12.8, N−CH_2−CH (isomer 2). ^{51}V NMR (CD_3OD, (integral)): δ −449 (1.00), −470 (0.57). Anal. Calcd for $C_{20}H_{24}NO_6V$ (M = 425.36 g mol^{-1}): C, 56.48; H, 5.69; N, 3.29. Found: C, 56.55; H, 5.56; N, 3.49.

[VO(OMe)$\mathbf{L'_B}$]. The complex was prepared in analogy to the procedure described above from 0.050 g (0.13 mmol) of $H_2\mathbf{L_B}$ and 0.031 g (0.13 mmol) of VO(O*i*Pr)$_3$ in 2 mL of CH_2Cl_2. Crystals suitable for the X-ray characterization were obtained from a saturated methanolic solution after it stood at −20 °C for 3 weeks. IR (KBr, cm^{-1}): ν(OH) 3450; ν(aryl-H) 3058, 3020; ν(C−H) 2983, 2928; ν(C═O) 1670; ν(C═C ring) 1490; δ(C−H) 1450, 1400; δ-(CH_3) 1375; δ(C−N) 1270; ν(C−O), ν(C−OC) 1150, 1061, 1032; ν(V═O) 961; δ(aryl-H) 741, 700. ^{1}H NMR ($CDCl_3$): δ 7.48−7.27 (m, 30H), 6.37−6.33 (dd, 3.2, 10.8, 1H, CH_2−C*H*(Ph)−OH (isomer 1)), 6.23−6.19 (dd, 3.4, 11, 1H, CH_2−C*H*(Ph)−OH (isomer 2)), 5.91−5.88 (dd, 4.5, 9.2, 1H, N−C*H*(Ph)−CH_2−), 5.60−5.54 (dd, 9.8, 11.5, 1H, CH(Ph)−CH_2−OH), 4.98 (s, 3H, V−O−CH_3 (isomer 1)), 4.70−4.66 (dd, 3.3, 13.0, 2H, N−CH_2−CH(Ph)), 4.47−4.43 (d, 18.3, 2H, N−CH_2−COOCH_3 (isomer 1)), 4.26−4.21 (d, 18.1, 2H, N−CH_2−COOCH_3 (isomer 2)), 4.09 (s, 3H, V−O−CH_3 (isomer 2)), 3.71 (s, 3H, −COOCH_3 (isomer 1)), 3.49−3.43 (dd, 9.0, 12.8, 3H, CH(Ph)−CH_2−OH, 3.24 (s, 3H, −COOCH_3 (isomer 2)), 3.00−2.94 (dd, 11.1, 12.9, 2H, N−CH_2−CH(Ph) (isomer 1)), 2.90−2.84 (dd, 11.1, 12.7, N−CH_2−CH(Ph) (isomer 2)). ^{51}V NMR (CD_2Cl_2, (integral)): δ −451 (1.00), −471 (1.49). Anal. Calcd for $C_{20}H_{24}NO_6V$ (M = 425.36 g mol^{-1}): C, 56.48, H, 5.69, N, 3.29. Found: C, 56.01; H, 5.10; N, 3.06.

[VO(O*i*Pr)$_2\mathbf{L_C}$] and [VO(O*i*Pr)($\mathbf{L_C}$)$_2$]. The complexes were prepared in analogy to the procedure described for the complex with $\mathbf{L_A}$ from 0.134 g (0.53 mmol) of $H\mathbf{L_C}$ and 0.064 g (0.26 mmol) of VO(O*i*Pr)$_3$ in 3 mL of CH_2Cl_2. Characterization of [VO-(O*i*Pr)$_2\mathbf{L_C}$] (in solution). ^{1}H NMR ($CDCl_3$): δ 7.45−7.28 (m, 12H), 5.80−5.68 (dd, 2H, CH_2−C*H*(Ph)−O), 5.29−5.20 (sept., 2H, V−O−C*H*(CH_3)$_3$), 4.10−4.02 (m, 5H, N−CH_2−COO(*t*Bu)), 3.15−3.03 and 2.98−2.81 (dd and dd, 3H and 3H, NH−CH_2−CH(Ph)O), 1.46 (s, 22H, CH_2−COO(CH_3)$_3$), 1.20−1.18 (d, 16H, (CH_3)$_2$CH−O−V). ^{51}V NMR (CD_2Cl_2 (integral)): δ −467 (1.0), −505 (0.4). Characterization of [VO(O*i*Pr)($\mathbf{L_C}$)$_2$] (isolated as a green solid, yield = 0.086 g (52%). IR (CH_2Cl_2, cm^{-1}): ν(N−H) 3375; ν(OH) 3100; ν(aryl-H) 3031, 2985; ν(C−H) 2933; ν(N−CH_2) 2837; ν(C═O) 1730; ν(C═C ring) 1600, 1491; δ(N−H) 1593; δ(C−H) 1450, 1391; δ(CH_3) 1372; ν(C−N) 1259, 1230; ν(C−O), ν(C−OC) 1160, 1135, 1042; ν(V═O) 948; δ(Aryl-H) 750, 700; ν(M−O) 650. Anal. Calcd for $C_{31}H_{47}N_2O_8V$ (M = 626.66 g mol^{-1}): C, 59.42; H, 7.56; N, 4.47. Found C, 59.01; H, 7.10; N, 4.52.

[VO(O*i*Pr)$_2\mathbf{L_D}$], [VO(O*i*Pr)($\mathbf{L_D}$)$_2$], and [VO(OMe)$\mathbf{L^*_D}$]. [VO-(O*i*Pr)$_2\mathbf{L_D}$] and [VO(O*i*Pr)($\mathbf{L_D}$)$_2$] were prepared in analogy to the respective complexes with $\mathbf{L_A}$ by reaction of 0.163 g (0.65 mmol) of ligand $\mathbf{L_D}$ and 0.077 g (0.32 mmol) of VO(O*i*Pr)$_3$ in 3 mL of CH_2Cl_2. [VO(O*i*Pr)$_2\mathbf{L_D}$] could not be isolated in pure form. Characterization of [VO(O*i*Pr)$_2\mathbf{L_D}$]. ^{1}H NMR ($CDCl_3$): δ 7.47−7.28 (m, 20H), 4.38−4.34 (dd, 5.5, 10.3, 2H, CH(Ph)−CH_2−OH), 4.27−4.22 (t, 10.6, 1H, NH−C*H*(Ph)−CH_2), 4.04−3.96 (m, 2H, NH−CH_2−COO*t*Bu), 3.98−3.71 (dd, 4.1, 8.1, 4H, CH(Ph)−CH_2−OH), 3.62−3.57 (t, 9.1, 2H, NH−C*H*(Ph)−CH_2), 3.32−3.13 (dd, 17.3, 39.5, 4H, NH−CH_2−COO*t*Bu), 1.43 (s, 27H, −COO*t*Bu), 1.22−1.20 (d, 6H, (CH_3)$_2$CH−OH). ^{51}V NMR ($CDCl_3$ (integral)): δ −450 (1.10), −479 (1.16), −520 (1.00). Characterization of [VO-(O*i*Pr)($\mathbf{L_D}$)$_2$] (green solid, yield = 0.093 g (47%)). IR (KBr, cm^{-1}): ν(N−H), ν(OH) 3381; ν(aryl-H) 3056, 2981; ν(C−H) 2930; ν-(N−CH_2) 2832; ν(C═O) 1739; ν(C═C ring) 1605, 1494; δ(N−H) 1560; δ(C−H) 1455; δ(CH_3) 1370; ν(C−N) 1266, 1230; ν(C−O), ν(C−OC) 1155, 1106, 1028; ν(V═O) 909; δ(aryl-H) 741, 695; ν(M−O) 648.

For the preparation of [VO(HOMe)(OMe)$\mathbf{L^*_D}$], 0.10 g (0.40 mmol) of $H\mathbf{L_D}$ was dissolved in 5 mL of CH_2Cl_2, and the mixture was treated with 16.28 g (0.143 mol) of trifloroacetic acid in 4 mL of CH_2Cl_2 under N_2. The solvents were evaporated in vacuo, and the residue was washed with 1:1 diethyl ether/petrol ether. The resulting ammonium salt of $\mathbf{L^*_D}$was converted to the potassium salt by addition of 1 M K_2CO_3 (pH adjustment to 8), and it was separated from CF_3CO_2K by gel chromatography on Sephadex G-10, using 1:2:1 water/ethanol/acetone. Yield of $K\mathbf{L^*_D}$ was 0.021 g (22%). $K\mathbf{L^*_D}$ was dissolved in 3 mL of anhydrous methanol and

treated dropwise with 0.018 g (0.073 mmol) of VO(O*i*Pr)$_3$. [VO(HOMe)(OMe)$\mathbf{L_D^*}$] was obtained as a yellow solution. IR (MeOH, cm^{-1}): ν(OH) 3367; ν(aryl-H) 2985, 2946; ν(C−H), ν(O−CH$_3$) 2870, 2833; ν_{as}(COO$^-$) 1678; δ(N−H) 1569; δ(C−H) 1449; ν_s(COO$^-$) 1367; ν(C−N) 1183; ν(C−O) 1122, 1054, 1032; ν(V═O) 916; δ(Aryl-H) 734; ν(M−O) 646. ^{51}V NMR (CDCl$_3$): δ −544.

[VO(OMe)$\mathbf{L_E^*}$]. The complex was prepared by reacting 0.070 g (0.335 mmol) of ligand H$\mathbf{L_E^*}$ with 0.082 g (0.335 mmol) of VO(O*i*Pr)$_3$ in 4 mL of absolute methanol. The brown-green precipitate was filtered off, washed with CH_2Cl_2, and dried in vacuo. Yield: 0.043 g (42%). IR (KBr, cm^{-1}): ν(OH) 3435; ν(aryl-H) 2968; ν(C−H) 2926; ν(N−CH$_2$) 2802; ν_{as}(COO$^-$) 1641; ν(C═C ring) 1496; δ(C−H) 1455; ν_s(COO$^-$) 1377; ν(C−N) 1248; ν(C−O) 1156, 1047; ν(V═O) 967; δ(aryl-H) 760, 703; ν(M−O) 560. ^{1}H NMR (CDCl$_3$): δ 7.40−7.26 (m, 5H), 4,54−4,42 (dd, 1H, CH$_2$−C*H*(Ph)−OV), 3.99 (s, 3H, V−O−C*H*$_3$), 3.25 (s, 2H, NH−C*H*$_2$−COO(*t*Bu), 2.86−2.80 and 2.61−2.56 (dd and dd, 1H and 1H, NH−C*H*$_2$−CH(Ph)OV), 2.25 (s, 3H, N−C*H*$_3$), 1.10 (d, 17H, C*H*$_3$−OH). ^{51}V NMR (CD_2Cl_2, (integral)): δ −448 (1.7), −465 (2.8), −557 (1.2). Anal. Calcd for $C_{12}H_{16}NO_5V$ (M = 305.20 g mol^{-1}): C, 47.22; H, 5.28; N, 4.59. Found: C, 48.10; H, 6.01; N, 4.06.

Acknowledgment. This work was supported by the Deutsche Forschungsgemeinschaft (Graduate School 611 and Grant RE 431/20-1).

Supporting Information Available: Characterization of the ligands H$_2\mathbf{L_A}$, H$_2\mathbf{L_C}$, and H$\mathbf{L_D}$. This material is available free of charge via the Internet at http://pubs.acs.org. Structures have been deposited with the Cambridge Crystallographic Data Centre (http://www.ccdc.cam.ac.uk; CCDC numbers 274801 (H$\mathbf{L_C}$), 245952 (H$\mathbf{L_D}$), CCDC-263138 (H$\mathbf{L_E^*}$·H$_2$O), and 246157 ([VO(OMe)($\mathbf{L_B'}$)])).

IC061534P